Bi-directional DFEs for Plastic Optical Fiber based In-vehicle Infotainment System at 2-3Gbit/s

Yixuan Wang
University Stuttgart
Institute of Telecommunications
Stuttgart, Germany +49711-68567925
Email: ywang@inue.uni-stuttgart.de

Lukas Mauch
University Stuttgart
Stuttgart, Germany +49711-91290545
Email: lukasmauch@googlemail.com

Joachim Speidel
University Stuttgart
Institute of Telecommunications
Stuttgart, Germany +49711-68568017
Email: speidel@inue.uni-stuttgart.de

***Abstract*—This paper investigates three types of adaptive bi-directional decision feedback equalizers (BiDFE) for the plastic optical fiber (POF) based high speed in-vehicle transmission for infotainment applications. We show that 2-3Gbit/s transmission speed can be reached with a 10m fiber length, using an light emitting diode (LED). BiDFE utilizes a forward DFE and a reverse DFE to equalize the received sequence and the time-reversed replica, and provides two decided symbol sequences. It uses then an arbitrator to choose from the two, the one which better explains the received sequence. Benefiting from the use of a reverse DFE, BiDFE can be superior to conventional DFE. Its performance is suboptimal compared to a posterior equalizer, but it is less complicated. Among the various BiDFE proposals, the bi-directional arbitrated DFE (BAD) and the trellis-based conflict resolution (TBCR) algorithm are specially considered in this paper. The simulation results show that they surpass conventional DFE by 1.5dB at bit error rate (BER) of 10^{-3} for a 3Gbit/s transmission. However, both algorithms have shortages and their performances can be improved by a novel equalization scheme proposed by this paper, named as the trellis-based BiDFE (TB-BiDFE). TB-BiDFE outperforms conventional DFE by 2dB at BER of 10^{-3}, and TBCR by 1dB at BER of 10^{-6} for a 3Gbit/s transmission. It has also a moderate complexity.**

I. INTRODUCTION

Future automobile applications, such as parallel transmission of HD-videos or side and front view cameras, demand high speed in-vehicle communication networks with Gbit/s data rate. However, the nowadays in-vehicle MOST150 optical physical layer provides only 150Mbit/s speed. Upgrading the optical layer to the Gbit/s range by glass fibers and lasers is more expensive, compared to the use of sophisticated electrical transmitter and receiver signal processing techniques, on the basis of existing optical network with plastic optical fiber (POF) and light emitting diode (LED).

In [1], a 3Gbit/s transmission is considered by using decision feedback equalizer (DFE) and Tomlinson Harashima precoding (THP) at high signal-to-noise ratio (SNR) conditions. Now the challenge is, how to achieve similar performances with lower SNRs and moderate complexity. Due to the very insufficient channel bandwidth of about 135MHz, high order modulation scheme has to be used. Thus, the Viterbi equalizer is not adequate because its complexity increases exponentially with the modulation order. In this paper, we introduce bi-directional DFE (BiDFE) in the electronic part of the receiver as a solution for the high bit rate transmission. It will be shown that it has moderate complexity as well as superior performance than the solutions in [1].

BiDFE operates with two DFEs: a forward DFE for equalizing the received sequence, and a reverse DFE for equalizing the time-reversed replica. It generates some sort of receive diversity artificially: the time-reversal operation makes errors in a forward and a reverse DFE to propagate in opposite directions, and most of the erroneous locations in the two DFEs are different. When the two DFEs have different decisions, an arbitrator has to choose the one which produces minimum squared Euclidean distance to the received sequence. By doing so, BiDFE can significantly mitigate the error propagation [2] and outperform the conventional DFE.

This paper first investigates the bi-directional arbitrated DFE (BAD) [3]. BAD does arbitration in a window around each conflicting DFE decision and requires some computational load. The trellis-based conflict resolution (TBCR) BiDFE [4], which is known for its lower computational complexity than BAD, is investigated thereafter. However, since both schemes provide only two estimates for the received sequence, we look into the problem how more estimates can be generated for improving the performance. As a result, a novel trellis-based algorithm (TB-BiDFE) is suggested. It reconstructs more than two estimates for the received sequence using a trellis diagram. We show that this method can outperform BAD and TBCR.

The remaining part of this paper is organized as follows: Section II models the MOST150 optical layer and the complete transmission system. In Section II, BAD, TBCR and the proposed TB-BiDFE algorithm are introduced in details. The simulation results are presented in Section IV. The last section concludes the paper.

II. SYSTEM MODEL

Fig. 1 depicts the considered system block diagram. Here, 8PAM and non-coherent optical demodulation with a photo-diode (PD) is applied. The impulse response of the equivalent base-band channel, measured from the electrical input to output, is indicated as h. Additive white Gaussian noise (AWGN) is an adequate noise model for the POF channel. Strong inter-symbol-interference (ISI) is caused by insufficient transmission bandwidth. To ensure a robust transmission, a BER between 10^{-3} and 10^{-4} is desired at the output of the

978-1-4673-1881-5/12/$31.00 ©2012 IEEE

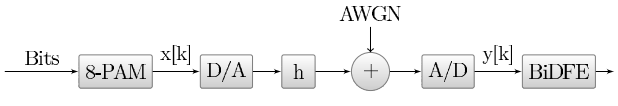

Fig. 1. System block diagram

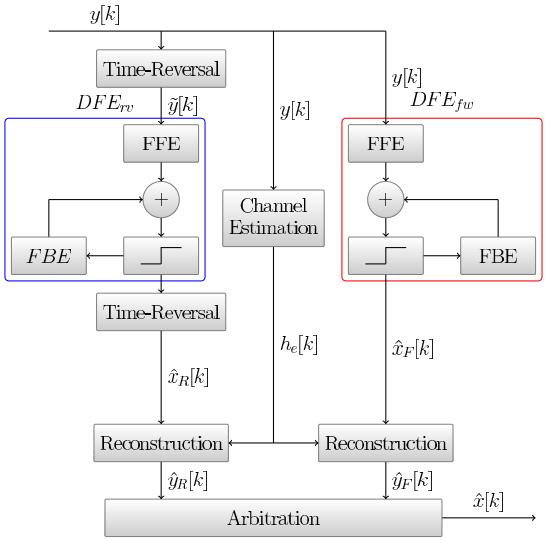

Fig. 2. Architecture of BiDFE

BiDFE. Then, Reed-Solomon (RS) encoding/decoding can be used to decrease the BER to 10^{-9} and below.

A. Optical Channel Model

The considered optical layer is a cascade of a LED, a 10m POF and a PD. According to the MOST150 specification, the optical layer can be modeled by its electrical equivalent baseband transfer function, which is a Gaussian low-pass filter:

$$H_a(f) = Ae^{-2(\pi\sigma f)^2} e^{-j2\pi f\tau L_{pof}}; \tag{1}$$

where L_{pof} is the fiber length, A is the linear fiber loss, $\sigma = \frac{0.132}{B}$ is the standard deviation, $B = 1009 \cdot \frac{L_{pof}}{m}^{-0.8747}$ MHz is the 3dB bandwidth, and $\tau = 4.97 \cdot 10^{-9}$ s/m. For a 10m POF, the 3dB bandwidth is 135MHz.

B. Receiver Architecture

The investigated BAD, TBCR and our proposed TB-BiDFE, share the same architecture, whose functional block diagram is shown in Fig. 2. It consists of four stages:

1) Equalization stage:
Equalization is done in parallel by a forward DFE and a reverse DFE, indicated as DFE_{fw} and DFE_{rv} respectively. Throughout this paper, a DFE contains a feedforward equalizer (FFE) and a feedback equalizer (FBE) part. The 8PAM symbols are transmitted in blocks, blocks are processed independently and one block is indicated as $x = \{x[k], k = 0, ..., N-1\}$. The input of the forward DFE is the received symbol sequence $y = \{y[k], k = 0, ..., N_y - 1\}$, with:

$$y[k] = x[k] * h[k] + n[k], \tag{2}$$

where $h = \{h[k], k = 0, ..., L_c - 1\}$ is the sampled (symbol-spaced) equivalent electrical channel impulse response corresponding to (1), $n[k]$ is the sampled AWGN and $N_y = N + L_c - 1$. At the reverse DFE, y is first reversed in time into $\tilde{y}$, where $\tilde{}$ stands for the time-reversal operation. So,

$$\begin{aligned} \tilde{y}[k] &= y[N_y - k - 1] \\ &= x[N_y - k - 1] * h[N_y - k - 1] + ... \\ &\quad n[N_y - k - 1] \\ &= \tilde{x}[k] * \tilde{h}[k] + \tilde{n}[k]. \end{aligned} \tag{3}$$

(3) well explains the time-reversal operation: reversing the received sequence is equivalent to reversing the transmitted sequence and the channel impulse response before the convolution [5], and the noise. Accordingly, taps of the reverse DFE are trained by the time-reversed channel impulse response. When a channel is asymmetric, taps of the two DFEs would have different values. The more asymmetric the channel is, the more diverse the values are. This consequently leads to different decided symbol sequences $\hat{x}_F = \{\hat{x}_F[k], k = 0, ..., N-1\}$ and $\hat{x}_R = \{\hat{x}_R[k], k = 0, ..., N-1\}$, and brings in the "receiving diversity". When a channel is symmetric, BiDFE doesn't benefit from the channel reversal. However, since noise in the received sequence is also reversed, which can be seen as independent appearing at the two DFEs, some diversity gain is obtained as well.

2) Channel estimation stage:
To acquire the estimated channel impulse response $h_e = \{h_e[k], k = 0, ..., L_e - 1\}$, which is needed for the reconstruction stage, maximum likelihood (ML) criterion is used in the training block for a precise estimation start, and least mean squares (LMS) algorithm is used afterwards for faster computational speed and adaptivity to the channel changes. When estimation works fine, L_e is close to L_c. We make this assumption throughout the paper, and use L_c instead of L_e in the following.

3) Reconstruction stage:
In this stage, h_e is convolved, depending on the BiDFE type, with either the complete decided symbol sequences $\hat{x}_F$ and $\hat{x}_R$ or some parts of them, to generate different estimates $\hat{y}_F$ and $\hat{y}_R$, for the received sequence y.

4) Arbitration stage:
Arbitration is done in the final step. Different types of BiDFEs differ mostly in here. However, the common idea is to choose from all candidate sequences/symbols, the one that best explains the received sequence, according to the arbitration criterion.

In this paper, the three considered BiDFEs share common stages 1 and 2, but differ at stages 3 and 4. Details are described in the next section.

III. BiDFE Algorithms

In this section, we review the BAD and TBCR algorithms, generalize the optimization problem, as well as formulate a

novel TB-BiDFE algorithm. All algorithms utilize adaptive DFEs, whose coefficients are updated with recursive least squares (RLS) and LMS algorithms. The channel estimation is also adaptive, as described in Section II.

A. Symbol-wise arbitrated BAD

The comprehensive operation of BAD was first described in [3]. The received sequence $y = \{y[k], k = 0, ..., N_y - 1\}$ is processed by stages 1 to 3 in Section II, to get the decided symbol sequences $\hat{x}_F = \{\hat{x}_F[k], k = 0, ..., N - 1\}$ and $\hat{x}_R = \{\hat{x}_R[k], k = 0, ..., N - 1\}$. Then $\hat{y}_F[k] = \hat{x}_F[k] * h_e[k]$ and $\hat{y}_R[k] = \hat{x}_R[k] * h_e[k]$ is reconstructed for $k = 0, ..., N_y - 1$.

For each $\hat{x}_F[k] = \hat{x}_R[k]$, the arbitrated final output $\hat{x}[k]$ is chosen from either one, as they are confirmed by both DFEs and are considered reliable. For each $\hat{x}_F[k] \neq \hat{x}_R[k]$ at time K, the squared Euclidean distances ξ_i^2 between y and $\hat{y}_i$, for i$\in$ {F,R}, are calculated in a window with length $2W + 1$ around the conflict symbol pair $\hat{x}_F[K]$ and $\hat{x}_R[K]$. Namely,

$$\xi_i^2{}_{[K-W]}^{[K+W]} = \sum_{min\{1,K-W\}}^{max\{K+W,N+L_c-1\}} |y[k] - \hat{y}_i[k]|^2, \quad \text{for i} \in \{\text{F,R}\} \tag{4}$$

where $[^{K+W}_{K-W}]$ identifies a time window from $K-W$ to $K+W$. The arbitrated final output $\hat{x}[k]$ is chosen as the one which has the smaller ξ_i^2. Finally, the decision rule for arbitration is:

$$\hat{x}[k] = \begin{cases} \hat{x}_F[k] \text{ or } \hat{x}_R[k], & \text{if } \hat{x}_F[k] = \hat{x}_R[k] \\ \hat{x}_F[k], & \text{if } \xi_F^2{}_{[k-W]}^{[k+W]} \leq \xi_R^2{}_{[k-W]}^{[k+W]} \\ \hat{x}_R[k], & \text{else} \end{cases} \tag{5}$$

B. Block-wise arbitrated TBCR

Because the symbol-wise arbitrated BAD yields a high computational complexity, a block-wise arbitrated TBCR with reduced complexity is proposed by [4]. The simplification comes from two considerations: first, consecutive identical symbol pairs in $\hat{x}_F$ and $\hat{x}_R$ produce identical reconstructed symbol pairs in $\hat{y}_F$ and $\hat{y}_R$, therefore making no contribution to the squared Euclidean distance. Reconstruction for these symbols is unnecessary. Second, the inconsistent symbol pairs in $\hat{x}_F$ and $\hat{x}_R$ tend to occur in bursts due to error propagation, which consequently cause contradictory bursts in $\hat{y}_F$ and $\hat{y}_R$. Instead of symbol-wise arbitration, the maximum likelihood sequence estimation (MLSE) can be adopted for reducing computational load. That is, while BAD calculates and compares $\xi_i^2{}_{[k-W]}^{[k+W]}$ for each $\hat{x}_F[k] \neq \hat{x}_R[k]$, TBCR calculates and compares $\xi_i^2{}_{[k_1]}^{[k_2]}$ for each $\hat{y}_F[k] \neq \hat{y}_R[k]$ in a block from k_1 to k_2. Note that $\hat{y}_F[k] \neq \hat{y}_R[k]$ must happen in a block-wise fashion with minimum length of L_c. This is due to the convolution delay, e.g., $\hat{x}_F[K] \neq \hat{x}_R[K]$ at time K would cause consecutive inconsistent $\hat{y}_F[k] \neq \hat{y}_R[k]$ from K to $K + L_c - 1$.

Therefore, we can divide $\hat{x}_F$ and $\hat{x}_R$ into conflict events and consistent blocks, which correspond to the inconsistent and consistent blocks in $\hat{y}_F$ and $\hat{y}_R$. A conflict event starts from the first contradict symbol pair in $\hat{x}_F$ and $\hat{x}_R$, and ends with $L_c - 1$ consecutive consistent pairs. It is used later on for the reconstruction. Whereas a consistent block indicates consecutively identical symbol pairs in $\hat{x}_F$ and $\hat{x}_R$ outside the conflict events. During arbitration, symbols in a consistent block are taken directly as final decisions. Fig. 3 gives an example of such a fragmentation for $L_c = 3$, where the consistent block is colored in blue and the conflict event is colored in red.

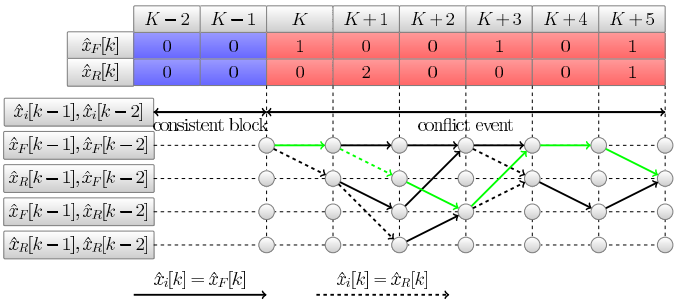

Fig. 3. Reconstruction and arbitration using a trellis diagram

TBCR algorithm can be summarized as [4]:

1) Apply stages 1 and 2 to the received sequence y, and get the decided symbol sequences $\hat{x}_F$ and $\hat{x}_R$.
2) Identify the conflict events and consistent blocks in $\hat{x}_F$ and $\hat{x}_R$.
3) For symbols in the consistent blocks, output them as the final decisions.
4) For each conflict event from k_1 to k_2, reconstruct $\hat{y}_F[^{k_2}_{k_1}]$ and $\hat{y}_R[^{k_2}_{k_1}]$. Compute $\xi_F^2[^{k_2}_{k_1}] = \sum_{k=k_1}^{k_2} |y[k] - \hat{y}_F[k]|^2$ and $\xi_R^2[^{k_2}_{k_1}] = \sum_{k=k_1}^{k_2} |y[k] - \hat{y}_R[k]|^2$, take the $\hat{x}_i[^{k_2}_{k_1}]$ which produces the smaller $\xi_i^2[^{k_2}_{k_1}]$ as the final decision.

C. Proposed block-wise arbitrated TB-BiDFE Algorithm

TBCR has one significant drawback, that is, a block with the minimum Euclidean distance is chosen as the final output, despite wrong symbols that may be contained in the block. When a conflict event gets larger, it is more likely that the chosen block contains wrong symbols. In order to overcome this drawback, we propose a new algorithm termed the trellis-based BiDFE (TB-BiDFE) algorithm.

Similar to TBCR, TB-BiDFE also partially reconstructs $\hat{y}$ and uses ξ^2 as a figure of merit for arbitration. Major difference is that for each conflict event $k_1 \leq k \leq k_2$, TBCR reconstructs two estimates $\hat{y}_F[k] = \hat{x}_F[k] * h_e[k]$ and $\hat{y}_R[k] = \hat{x}_R[k] * h_e[k]$; whereas TB-BiDFE reconstructs:

$$\begin{aligned} \hat{y}[k] \quad = \quad & \hat{x}_i[k] \cdot h_e[0] + \hat{x}_i[k-1] \cdot h_e[1] + \cdots \\ & + \hat{x}_i[k - L_c + 1] \cdot h_e[L_c - 1], \end{aligned} \tag{6}$$

with $\hat{x}_i[k] \in \{\hat{x}_F[k], \hat{x}_R[k]\}$, so $\hat{x}_F[k]$ and $\hat{x}_R[k]$ are mixed in (6). By doing so, TB-BiDFE can reconstruct at least 2 and at most 2^{L_c} different estimates $\hat{y}[k]$ for k inside a conflict event, which are more than those of TBCR, thus the drawback of TBCR is avoided. Note that the number of reconstructed $\hat{y}[k]$ is only related to the channel length L_c but not to the

modulation order of $\hat{x}[k]$, which makes TB-BiDFE simpler than the Viterbi algorithm.

When visualizing (6) by a trellis diagram, whose nodes represent 2^{L_c-1} combinations of $\{\hat{x}_i[k-1], \hat{x}_i[k-2], \cdots, \hat{x}_i[k-L_c+1]\}$, and branches stands for $\hat{x}_i[k]$, then the reconstruction progress of different $\hat{y}[k]$ is illustrated by paths on the trellis diagram.

An example is given in Fig. 3. There, 3PAM with symbol alphabet $\{0, 1, 2\}$ and a channel length $L_c = 3$ are assumed. First we partition $\hat{x}_F$ and $\hat{x}_R$ into a consistent block ($K-2 \leq k \leq K-1$, marked in blue) and a conflict event ($K \leq k \leq K+5$, marked in red). Symbols belonging to the consistent block are output directly as final decisions. Symbols from the conflict event are taken for reconstruction. According to (6), we get $\hat{y}[k] = \hat{x}_i[k]\cdot h_e[0] + \hat{x}_i[k-1]\cdot h_e[1] + \hat{x}_i[k-2]\cdot h_e[2]$. The corresponding trellis diagram has thus $2^{L_c-1} = 4$ states, which are $S_1 = \{\hat{x}_F[k-1], \hat{x}_F[k-2]\}$, $S_2 = \{\hat{x}_R[k-1], \hat{x}_F[k-2]\}$, $S_3 = \{\hat{x}_F[k-1], \hat{x}_R[k-2]\}$ and $S_4 = \{\hat{x}_R[k-1], \hat{x}_R[k-2]\}$. If $\hat{x}_F[k] \neq \hat{x}_R[k]$, a node is split into two branches, each stands for $\hat{x}_i[k] = \hat{x}_F[k]$ (solid line) or $\hat{x}_i[k] = \hat{x}_R[k]$ (dashed line). If $\hat{x}_F[k] = \hat{x}_R[k]$, then $\hat{x}_i[k] = \hat{x}_F[k]$.

The paths start from state S_1, since the previous consistent block makes $\{\hat{x}_i[K-1], \hat{x}_i[K-2]\} = \{\hat{x}_F[K-1], \hat{x}_F[K-2]\}$. For $K \leq k \leq K+1$, $\hat{x}_F[k] \neq \hat{x}_R[k]$, each node is split into two for two times. Till $k = K+1$, the four paths on the trellis diagram indicate $\{\hat{x}[K+1], \hat{x}[K], \hat{x}[K-1]\} = \{0, 1, 0\}$, $\{0, 0, 0\}$, $\{2, 1, 0\}$ and $\{2, 0, 0\}$ respectively, and thus indicate four different reconstructed $\hat{y}[K+1]$. For $k = K+2$, $\hat{x}_i[k] = \hat{x}_F[k]$. For $K+4 \leq k \leq K+5$, $\hat{x}_F[k] = \hat{x}_R[k]$, paths take $L_c - 1$ steps to merge again. During creation of the paths, the path costs, which are the squared Euclidean distances between the reconstructed $\hat{y}$ and the received sequence y, are computed. When several paths merge at one node, paths with higher path costs are abandoned immediately. In the end, the path which has the lowest path cost survives and its corresponding $\hat{x}$ is the final output for the conflict event. E.g., the survived green path in Fig. 3 represents the final decision output $\hat{x}_K^{[K+5]}$ for the conflict event is $\{1, 2, 0, 1, 0, 1\}$.

TB-BiDFE algorithm is summarized as:

1) Apply stages 1 and 2 to the received sequence y, and get the decided symbol sequences $\hat{x}_F$ and $\hat{x}_R$.
2) Identify the conflict events and consistent blocks in $\hat{x}_F$ and $\hat{x}_R$.
3) For symbols in the consistent blocks, output them as the final decisions.
4) For each conflict event from k_1 to k_2, use the trellis diagram to reconstruct $\hat{y}[k]$ using $\hat{x}_i[k] \in \{\hat{x}_F[k], \hat{x}_R[k]\}$. Find out the $\hat{y}_{k_1}^{[k_2]}$ which has the minimum $\xi^2{}_{k_1}^{[k_2]}$, output its corresponding $\hat{x}_{k_1}^{[k_2]}$ as the final output.

IV. Simulation Results

Simulations of BER as a function of SNR are presented in this section. The SNR ranges from 20.4dB to 59.5dB based on a given optical link budget [1]. The area-of-interest for BER is $10^{-3} \sim 10^{-4}$, then RS coding can be adopted to decrease the BER to 10^{-9} and below. The transmission is on a block-wise basis to ensure that the time-reversal operation is applicable.

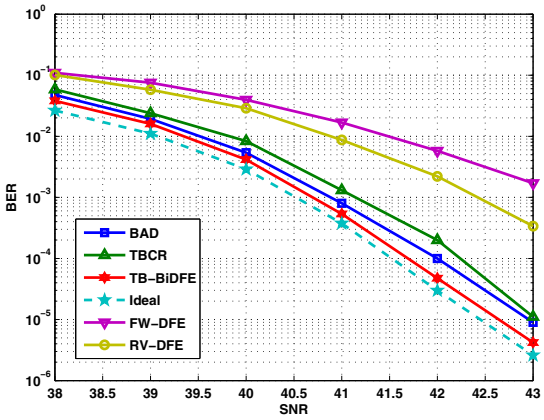

Fig. 4. Symbol-spaced BiDFEs at 3Gbit/s, $n_f = 15$.

The DFEs in the receiver are either symbol-spaced or fractionally-spaced with twice the symbol rate. Their tap weights are updated by RLS or LMS algorithm. The RLS algorithm jointly optimizes the forward and feedback weights in a training block and ensures rapid tap convergence. The LMS algorithm is adopted thereafter for faster simulation speed. Due to the slow fading nature of the optical channel, a small step-size is sufficient for the channel tracking.

To identify the performance for different schemes, BiDFEs, BAD, TBCR and TB-BiDFE are compared with each other, as well as with a theoretical ideal case, which assumes that an arbitrator has full knowledge of the original transmitted symbol $x[k]$. Its arbitration rule is:

$$\hat{x}[k] = \begin{cases} \hat{x}_F[k], & \text{if } |\hat{x}_F[k] - x[k]| \leq |\hat{x}_R[k] - x[k]| \\ \hat{x}_R[k], & \text{else} \end{cases} \tag{7}$$

The following simulation parameters are used in this section: modulation scheme: 8PAM; bandwidth of the equivalent base-band channel: 135MHz; symbol block length N: 3200; W for BAD arbitration: 10; the tap number of the feed-forward and the feedback part of a DFE: n_f.

A. Symbol-spaced BiDFEs

Fig. 4 demonstrates a 3Gbit/s transmission over the given channel using symbol-spaced BiDFEs. The different performances of the forward and the reverse DFE come from the fact that the channel is asymmetric after symbol-spaced sampling. In comparison with the reverse DFE, BAD and TBCR require 1.5dB and TB-BiDFE requires 2dB less SNR at BER $= 10^{-3}$. A lower bound for the BER, indicating the ideal case, is given by employing (7). The result shows that TB-BiDFE has the closest performance to the ideal case. BAD and TBCR perform a little worse.

B. Fractionally-spaced BiDFEs

Fig. 5 and Fig. 6 present the BER curves for 2Gbit/s and 3Gbit/s transmission with $T/2$ fractionally-spaced BiDFEs.

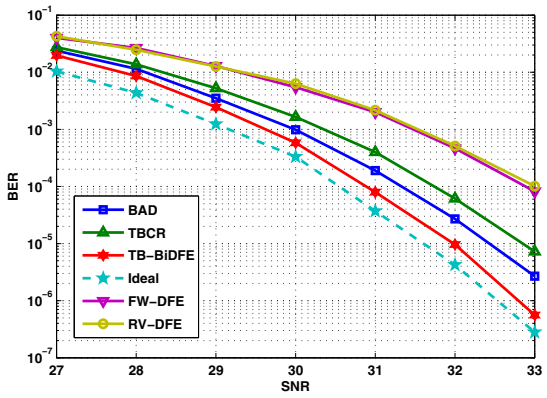

Fig. 5. Fractionally-spaced BiDFEs at 2Gbit/s, $n_f = 17$.

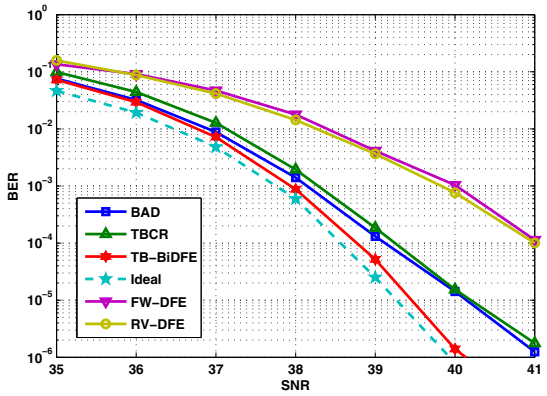

Fig. 6. Fractionally-spaced BiDFEs at 3Gbit/s, $n_f = 29$.

For BER between 10^{-3} and 10^{-4}, both figures show that TB-BiDFE has a SNR gain of $2 \sim 2.2$dB over conventional DFE, whereas BAD and TBCR have only $1 \sim 1.8$dB SNR gain. At 2Gbit/s, TB-BiDFE outperforms BAD by 0.4dB and TBCR by 0.8dB at BER $= 10^{-4}$. At 3Gbit/s, the BER of 10^{-3} is achieved for all BiDFEs with SNR around 38.2dB. Compared to the symbol-spaced BiDFEs in Fig. 4, which require SNR $= 40 \sim 41.5$dB for the same BER, a gain of about 3dB is obtained by oversampling.

We also observe from both figures that the distance between the BER curve of TB-BiDFE and the curves of BAD and TBCR becomes larger with decreasing BER. At 2Gbit/s, TB-BiDFE outperforms TBCR by 1dB at BER $= 10^{-5}$, and the same gain is achieved with 3Gbit/s at BER $= 10^{-6}$.

C. Comparison of computational complexity

An estimation of computational complexity is given by the number of additions and multiplications, which are required to process a symbol block. For TBCR and TB-BiDFE, this figure depends especially on the mean number N_{contr} of conflict events in a symbol block and the mean length L_{contr} of the conflict events.

The complexities of BAD and TBCR are listed in Table I. To estimate the maximum complexity of TB-BiDFE, we take into account that, $\hat{x}_F$ and $\hat{x}_R$ contradict consecutively with each other in a conflict event except for the last $L_c - 1$ symbols. An example for this case is the $\hat{x}_F[_K^{K+5}]$ and $\hat{x}_R[_K^{K+5}]$ in Fig. 3, but with $\hat{x}_F[K+2] \neq \hat{x}_R[K+2]$. The maximum computational complexity of TB-BiDFE is also listed in Table I.

TABLE I
COMPUTATIONAL COMPLEXITIES

Algorithm	Number of additions
BAD	$2N(L_c-1)+2N_{contr}(4W+1)$
TBCR	$2N_{contr}(L_{contr}L_c+L_{contr}-1)$
TB-BiDFE	$N_{contr}(2^{L_c}((L_c+1)(L_{contr}-2L_c)+4L_c)-4)$
Algorithm	**Number of multiplications**
BAD	$2NL_c+2N_c(2W+1)$
TBCR	$2N_{contr}L_{contr}(L_c+1)$
TB-BiDFE	$N_{contr}2^{L_c}((L_c+1)(L_{contr}-2L_c)+4L_c)$

For a 3Gbit/s transmission in Fig. 4 with SNR$= 41.5$dB, $L_c = 6$, $W = 10$ and $N = 3200$, we get $N_{contr} = 3.7$, $L_{contr} = 38$ for TBCR and TB-BiDFE, and $N_{contr} = 104$ for BAD. The complexity of TB-BiDFE is similar to the complexity of BAD and is 25 times higher than the complexity of TBCR. For a smaller L_c, TBCR and TB-BiDFE even show similar complexities. The number of states used in TB-BiDFE is $2^{L_c-1} = 32$, whereas it amounts to $8^{L_c-1} = 32768$ in a Viterbi equalizer using 8PAM.

V. CONCLUSION

In this paper, BAD, TBCR and TB-BiDFE are investigated on a basis of the MOST150 optical channel. However, they can also be used for other kinds of channels. With theoretical analysis and simulations, their advantages and shortages are investigated. It is shown that all BiDFEs with few number of filter taps can effectively eliminate the ISI lasting up to several symbol duration. All BiDFEs present superior performances compared to conventional DFE. For the target BER between 10^{-3} and 10^{-4}, BiDFEs provide $1 \sim 2$dB performance gain over conventional DFEs at both 2 and 3Gbit/s.

To improve the performance of BAD and TBCR, a novel trellis-based algorithm – TB-BiDFE – is presented. By use of a trellis diagram, TB-BiDFE is able to generate more estimates for the received sequence than BAD and TBCR. For a 3Gbit/s transmission using fractionally-spaced DFEs, TB-BiDFE outperforms BAD and TBCR by 1dB at BER $= 10^{-6}$, while having a moderate complexity.

REFERENCES

[1] Y. Wang, "Investigation and Simulation of high speed Gigabit Transmission for POF based MOST Networks," *Elektronik Automotive (Special issue MOST)*, pp. 18–33, Apr. 2011.

[2] G. Wang, J.-P. Ebert, and R. Kraemer, "BAAD: Bidirectional Arbitrated Adaptive DFE," in *Sarnoff Symposium, 2006 IEEE*, Mar. 2006, pp. 1–4.

[3] J. Nelson, A. Singer, U. Madhow, and C. McGahey, "BAD: bidirectional arbitrated decision-feedback equalization," *IEEE Trans. Commun.*, vol. 53, no. 2, pp. 214–218, Feb. 2005.

[4] C. W. Wong, J. Shea, and Y. Lee, "Hard- and soft-output trellis-based conflict resolution for bidirectional decision feedback equalization," *IEEE Trans. Wireless Commun.*, vol. 8, no. 7, pp. 3780 –3788, Jul. 2009.

[5] J. Balakrishnan and J. Johnson, C.R., "Bidirectional decision feedback equalizer: infinite length results," in *Signals, Systems and Computers, 2001. Conference Record of the Thirty-Fifth Asilomar Conference on*, vol. 2, 2001, pp. 1450–1454.